candidate miRNAs in mouse (18). Similarly, our screening for miRNAs in human clinical specimens by mRAP resulted in the isolation of a set of candidate novel miRNAs that include many with no mouse orthologs either in our dataset or in the miRBase depository (S. Takada, Y. Yamashita, E. Berezikov, Y.L. Choi, S. Fujiwara, M. Enomoto, H. Hatanaka, H. Watanabe, M. Soda, R.H.A. Plasterk, E. Cuppen and H. Mano, manuscript submitted). It is thus likely that the mouse genome encodes additional miRNAs yet to be discovered.

Isolation of novel miRNAs has been attempted to date through a variety of approaches. Lagos-Quintana *et al.* (13) compared miRNA profiles among mouse organs by a conventional miRNA cloning procedure. They identified that three miRNAs are expressed in a tissue-specific manner; mmu-mir-1 in heart, mmu-mir-124a in brain and mmu-mir-122a in liver, all of which is in a very good agreement with our observation (see Figure 3A and Supplementary Table S5). On the other hand, Barad *et al.* (23) chose oligonucleotide microarrays to compare miRNA profiles among five human tissues. Again, they revealed a tissue-specific expression of hsa-miR-122a and hsa-miR-124a, which matches our results.

Mineno *et al.* (24) recently analyzed miRNA expression with the massively parallel signature sequencing (MPSS) technology among three developmental stages (9.5, 10.5 and 11.5 dpc) of mouse embryo. Many of their 'top 20 miRNA signatures' can be observed in our dataset. For instance, their result reveals that the expression of mmu-mir-199a was increased from 9.5 to 11.5 dpc of mouse embryo. Our data demonstrates that the augmentation of mmu-mir-199a expression further continues to 15.5–17.5 dpc (Supplementary Table S3) of embryo. Similarly, both of our and Mineno's data indicate that mmu-mir-19b is abundantly expressed at 9.5–11.5 dpc of mouse embryo (Supplementary Table S3). Additionally, one of the abundant novel miRNAs in our embryo dataset, Mmj_157, was also counted for many times as miRNA426 in the data of Mineno *et al.* There may be, however, some difference between these two datasets. One of the highly expressed miRNAs in mouse embryo, mmu-mir-124a, in our data are missed from that of Mineno *et al.* Our northern blot analysis in Figure 2B supports the expression of mmu-mir-124a in embryo.

To directly compare our mRAP data with those by other high-throughput methods, we then hybridized RNA from

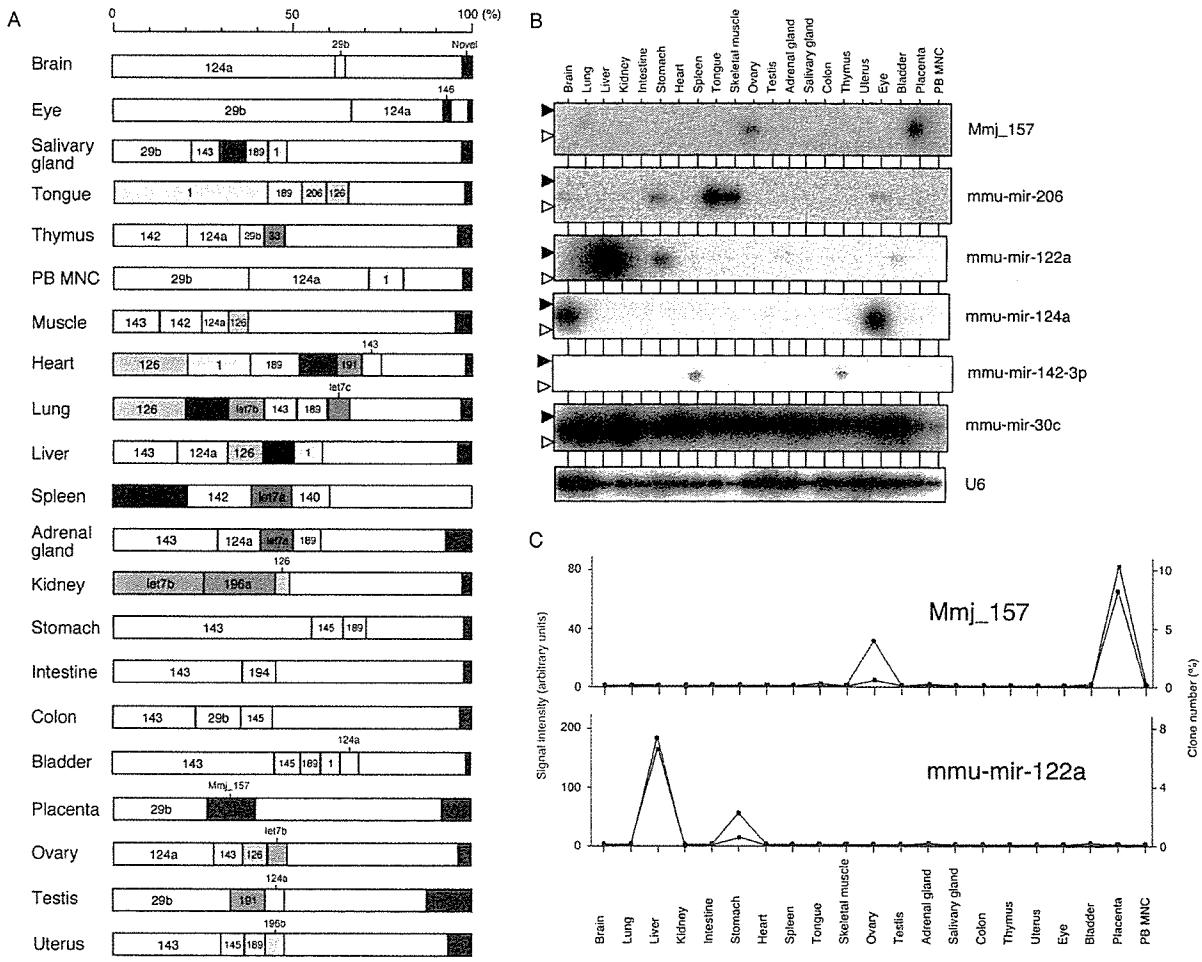

Figure 3. Expression profiles of miRNAs in adult mouse organs. (**A**) The percentage of each miRNA among the total miRNA population was calculated for the indicated organs of the adult mouse and is shown schematically as in Figure 2A. PB MNC, peripheral blood mononuclear cells. (**B**) Northern blot analysis of the Small-RNA fraction from the indicated adult mouse organs with probes specific for the indicated RNA species. (**C**) Expression levels of Mmj_157 or mmu-mir-122a in adult mouse organs as determined from the northern blot in (B) and from mRAP data.

Jurkat cell line to miRCURY LNA microarrays (Exiqon, Vedbaek, Denmark) to quantitate miRNA amounts. Hsa-miR-142, the most abundant miRNA in our Jurkat dataset (Supplementary Table S1), was indeed identified as one of the strongest signals in the array data (data not shown). However, with regard to another abundant miRNA hsa-miR-143 in our dataset, the microarray could give a hybridization signal only at the intensity of backgrounds (data not shown). Northern blot analysis clearly confirmed the expression of hsa-miR-143 in Jurkat cells (Supplementary Figure S1), supporting our mRAP data. Caution should thus be taken to estimate the miRNA profiles based on some type of microarrays.

We also quantitated the expression level of mmu-mir-122a, mmu-mir-185 and let-7-a with the TaqMan MicroRNA assay (Applied Biosystems) in mouse brain, liver and heart. Relative expression intensity of mmu-mir-122a to that of let-7-a was 1.056×10^{-4} for brain, 7.227 for liver and 1.230×10^{-4} for heart, indicating the liver-specific expression of mmu-mir-122a. On the other hand, the TaqMan assay revealed a weak but ubiquitous expression of mmu-mir-185; its relative expression level to that of let-7-a was 5.759×10^{-3} for brain, 3.816×10^{-3} for liver and 6.769×10^{-3} for heart. Both of these data are highly compatible with our dataset (Supplementary Table S5).

Given that mRAP is able to provide an miRNA profile with as few as 1×10^4 cells, it opens up the possibility of direct characterization of miRNAs in small amounts of tissue, such as those available for mouse embryos (as demonstrated in the present study) and fresh human specimens. Indeed, with mRAP, we have characterized miRNA profiles even for small papillary muscles of the human heart ventricle (S. Takada, R. Kaneda, E. Berezikov, Y. Yamashita, Y.L. Choi, S. Fujiwara, M. Enomoto, H. Hatanaka, H. Watanabe, M. Soda, R.H.A. Plasterk, E. Cuppen and H. Mano, manuscript submitted). Our present miRNA profiling in mouse has shown that such profiles vary markedly among tissues and developmental stages. An important application of mRAP will be determination of whether expression of miRNAs is associated with human disease by analysis of fresh human tissue specimens.

SUPPLEMENTARY DATA

Supplementary Data are available at NAR online.

ACKNOWLEDGEMENTS

The authors thank K. Nakamura for help in preparation of the manuscript. This work was supported in part by a grant for Third-Term Comprehensive Control Research for Cancer from the Ministry of Health, Labor and Welfare of Japan, and by a grant for 'High-Tech Research Center' Project for Private Universities: matching Fund Subsidy from the Ministry of Education, Culture, Sports, Science and Technology of Japan (2002–2006). E.B. was supported by the Horizon Breakthrough grant from the Netherlands Genomics Initiative. Funding to pay the Open Access publication charges for this article was provided by the Ministry of Education, Culture, Sports, Science and Technology, Japan.

Conflict of interest statement. None declared.

REFERENCES

1. Meister,G. and Tuschl,T. (2004) Mechanisms of gene silencing by double-stranded RNA. *Nature*, **431**, 343–349.
2. Bartel,D.P. (2004) MicroRNAs: genomics, biogenesis, mechanism and function. *Cell*, **116**, 281–297.
3. Abbott,A.L., Alvarez-Saavedra,E., Miska,E.A., Lau,N.C., Bartel,D.P., Horvitz,H.R. and Ambros,V. (2005) The let-7 MicroRNA family members mir-48, mir-84, and mir-241 function together to regulate developmental timing in *Caenorhabditis elegans*. *Dev. Cell*, **9**, 403–414.
4. Lee,R.C., Feinbaum,R.L. and Ambros,V. (1993) The *C. elegans* heterochronic gene lin-4 encodes Small-RNAs with antisense complementarity to lin-14. *Cell*, **75**, 843–854.
5. Bernstein,E., Kim,S.Y., Carmell,M.A., Murchison,E.P., Alcorn,H., Li,M.Z., Mills,A.A., Elledge,S.J., Anderson,K.V. and Hannon,G.J. (2003) Dicer is essential for mouse development. *Nature Genet.*, **35**, 215–217.
6. Chen,C.Z., Li,L., Lodish,H.F. and Bartel,D.P. (2004) MicroRNAs modulate hematopoietic lineage differentiation. *Science*, **303**, 83–86.
7. Lu,J., Getz,G., Miska,E.A., Alvarez-Saavedra,E., Lamb,J., Peck,D., Sweet-Cordero,A., Ebert,B.L., Mak,R.H., Ferrando,A.A. *et al.* (2005) MicroRNA expression profiles classify human cancers. *Nature*, **435**, 834–838.
8. Calin,G.A., Ferracin,M., Cimmino,A., Di Leva,G., Shimizu,M., Wojcik,S.E., Iorio,M.V., Visone,R., Sever,N.I., Fabbri,M. *et al.* (2005) A MicroRNA signature associated with prognosis and progression in chronic lymphocytic leukemia. *N. Engl. J. Med.*, **353**, 1793–1801.
9. Johnson,S.M., Grosshans,H., Shingara,J., Byrom,M., Jarvis,R., Cheng,A., Labourier,E., Reinert,K.L., Brown,D. and Slack,F.J. (2005) RAS is regulated by the let-7 microRNA family. *Cell*, **120**, 635–647.
10. Calin,G.A., Sevignani,C., Dumitru,C.D., Hyslop,T., Noch,E., Yendamuri,S., Shimizu,M., Rattan,S., Bullrich,F., Negrini,M. *et al.* (2004) Human microRNA genes are frequently located at fragile sites and genomic regions involved in cancers. *Proc. Natl Acad. Sci. USA*, **101**, 2999–3004.
11. Berezikov,E., Guryev,V., van de Belt,J., Wienholds,E., Plasterk,R.H. and Cuppen,E. (2005) Phylogenetic shadowing and computational identification of human microRNA genes. *Cell*, **120**, 21–24.
12. Bentwich,I., Avniel,A., Karov,Y., Aharonov,R., Gilad,S., Barad,O., Barzilai,A., Einat,P., Einav,U., Meiri,E. *et al.* (2005) Identification of hundreds of conserved and nonconserved human microRNAs. *Nature Genet.*, **37**, 766–770.
13. Lagos-Quintana,M., Rauhut,R., Yalcin,A., Meyer,J., Lendeckel,W. and Tuschl,T. (2002) Identification of tissue-specific microRNAs from mouse. *Curr. Biol.*, **12**, 735–739.
14. Ewing,B. and Green,P. (1998) Base-calling of automated sequencer traces using phred. II. Error probabilities. *Genome Res.*, **8**, 186–194.
15. Hofacker,I.L. (2003) Vienna RNA secondary structure server. *Nucleic Acids Res.*, **31**, 3429–3431.
16. Thompson,J.D., Higgins,D.G. and Gibson,T.J. (1994) CLUSTAL W: improving the sensitivity of progressive multiple sequence alignment through sequence weighting, position-specific gap penalties and weight matrix choice. *Nucleic Acids Res.*, **22**, 4673–4680.
17. Bonnet,E., Wuyts,J., Rouze,P. and Van de Peer,Y. (2004) Evidence that microRNA precursors, unlike other non-coding RNAs, have lower folding free energies than random sequences. *Bioinformatics*, **20**, 2911–2917.
18. Berezikov,E., van Tetering,G., Verheul,M., van de Belt,J., van Laake,L., Vos,J., Verloop,R., van de Wetering,M., Guryev,G., Takada,S. *et al.* (2006) Many novel mammalian microRNA candidates identified by extensive cloning and RAKE analysis. *Genome Res.*, in press.
19. Kloosterman,W.P., Wienholds,E., de Bruijn,E., Kauppinen,S. and Plasterk,R.H. (2006) *In situ* detection of miRNAs in animal embryos using LNA-modified oligonucleotide probes. *Nature Meth.*, **3**, 27–29.
20. Chenchik,A., Zhu,Y.Y., Diatchenko,L., Li,R., Hill,J. and Siebert,P.D. (1998) In Siebert,P.D. and Larrick,J. (eds.), *Gene Cloning and Analysis by RT–PCR*. BioTechniques Books, MA, pp. 305–319.
21. Ambros,V., Bartel,B., Bartel,D.P., Burge,C.B., Carrington,J.C., Chen,X., Dreyfuss,G., Eddy,S.R., Griffiths-Jones,S., Marshall,M. *et al.* (2003) A uniform system for microRNA annotation. *RNA*, **9**, 277–279.

22. Berezikov,E., Cuppen,E. and Plasterk,R.H. (2006) Approaches to microRNA discovery. *Nature Genet.*, **38**, S2–S7.
23. Barad,O., Meiri,E., Avniel,A., Aharonov,R., Barzilai,A., Bentwich,I., Einav,U., Gilad,S., Hurban,P., Karov,Y. *et al.* (2006) MicroRNA expression detected by oligonucleotide microarrays: system establishment and expression profiling in human tissues. *Genome Res.*, **14**, 2486–2494.
24. Mineno,J., Okamoto,S., Ando,T., Sato,M., Chono,H., Izu,H., Takayama,M., Asada,K., Mirochnitchenko,O., Inouye,M. *et al.* (2006) The expression profile of microRNAs in mouse embryos. *Nucleic Acids Res.*, **34**, 1765–1771.

Available online at www.sciencedirect.com
SCIENCE DIRECT®
Leukemia Research 30 (2006) 1105–1112
Leukemia Research
www.elsevier.com/locate/leukres

Expression of the myeloperoxidase gene in AC133 positive leukemia cells relates to the prognosis of acute myeloid leukemia

Jun Taguchi [a], Yasushi Miyazaki [a,*], Chizuko Tsutsumi [a], Yasushi Sawayama [a], Koji Ando [a], Hideki Tsushima [a], Takuya Fukushima [a], Tomoko Hata [a], Shinichiro Yoshida [b], Kazutaka Kuriyama [c], Sumihisa Honda [d], Itsuro Jinnai [a], Hiroyuki Mano [e], Masao Tomonaga [a]

[a] *Department of Hematology and Molecular Medicine Unit, Atomic Bomb Disease Institute, Nagasaki University Graduate School of Biomedical Sciences, 1-12-4 Sakamoto, Nagasaki 852-8523, Japan*
[b] *Department of Internal Medicine, Nagasaki National Medical Center, 2-1001-1 Ohmura, Nagasaki 856-8562, Japan*
[c] *School of Health Sciences, University of the Ryukyus, Nishihara, Okinawa 903-0215, Japan*
[d] *Department of Radiation Epidemiology, Atomic Bomb Disease Institute, Nagasaki University Graduate School of Biomedical Sciences, 1-12-4 Sakamoto, Nagasaki 852-8523, Japan*
[e] *Divisions of Functional Genomics, Jichi Medical School, 3311-1 Minamikawachi-machi Yakushiji, Kawachi-gun, Tochigi 329-0498, Japan*

Received 15 October 2005; received in revised form 30 December 2005; accepted 30 December 2005
Available online 2 February 2006

Abstract

We previously reported that the percentage of myeloperoxidase (MPO) positive blasts had a prognostic impact on survival of patients with acute myeloid leukemia (AML). To extend this observation, we quantitatively measured the level of the MPO gene in AC133 positive leukemia cells that would contain a putative AML stem/progenitor compartment. AML cases were divided into the MPO gene high (MPOg-H) and MPO gene low (MPOg-L) groups. Only patients belonging to the MPOg-H group had a favorable chromosomal translocation, t(8;21), and having no morphological dysplasia that was associated with MPOg-L. The difference in the survival of MPOg-H and MPOg-L was statistically meaningful, demonstrating the possible prognostic impact of the expression of MPO gene in AC133 positive leukemia cells.

Keywords: Myeloperoxidase; Gene expression; AC133; Acute myeloid leukemia; Prognostic factor

1. Introduction

Myeloperoxidase (MPO) is an enzyme exclusively expressed in hematopoietic cells committed to myeloid lineage [1–4]. Based on its specific expression in normal myeloid cells, both the enzymatic activity and the presence of MPO protein in leukemia blasts have been used for the diagnosis of acute myeloid leukemia (AML) by the French–American–British (FAB) group [5] as prime markers for the myeloid lineage of leukemia blasts.

Apart from its role in diagnosis, MPO in leukemia blasts was also shown to have a prognostic value by several groups [6–8]. In our recent report [8], AML patients with high percentage of MPO positive blasts (>50% of blasts are MPO activity positive, blast MPOa-H group) defined by routine cytochemical staining had a significantly better outcome compared to the low MPO activity positive blast group (MPO activity positive blasts ≤ 50%, blast MPOa-L). Multivariate analysis picked up the percentage of MPO positive blast as an independent prognostic factor along with karyotypes, WBC count at diagnosis and age. Considering that most of AML cases with favorable karyotyes, such as t(8;21) or inv(16) belong to the blast MPOa-H group (83 out of 88 cases in our previous report), it is suggested that MPO is one of the proteins highly expressed in leukemia blasts of AML cases with favorable prognosis by conventional chemotherapy.

Abbreviations: AML, acute myeloid leukemia; FAB, French–American–British; GAPDH, glyceraldehyde-3-phosphate dehydrogenase; MLD, multilineage myelodysplasia; MPO, myeloperoxidase; PBS, phosphate-buffered saline; WBC, White blood cell

* Corresponding author. Tel.: +81 95 849 7111; fax: +81 95 849 7113.
E-mail address: y-miyaza@net.nagasaki-u.ac.jp (Y. Miyazaki).

0145-2126/$ – see front matter © 2006 Elsevier Ltd. All rights reserved.
doi:10.1016/j.leukres.2005.12.012

Recent studies on leukemia cell populations revealed that a hierarchy of differentiation exists in AML blasts consisting of leukemia stem/progenitor cells and maturing blast cells. AML stem cells that are transplantable into NOD-SCID mice constitute a small proportion of leukemia cell population and they bear surface markers usually found on normal hematopoietic stem cells, such as CD34 and AC133 (CD133, PROMININ1 [PROM1]) [9–14]. CD133 expression has been demonstrated not only on hematopoietic stem cells shown by the reconstitution of hemtopoiesis using transplantation model but also on other tissue cells, such as undifferentiated epithelium and fetal brain neural stem cells. It is suggested that CD133 could be expressed on the surface of various stem/progenitor cells [15]. These antigens were successfully used to select leukemia stem cells to analyze, for example, the gene expression profile in hematopoietic stem cells or leukemia stem cells [9,14–17]. We have also examined the expression of more than 12,000 genes in AC133 positive leukemia cells, and compared the gene expression profiles between AML cases with and without morphological dysplasia (AML with multilineage dysplasia, AML/MLD and AML/non-MLD), demonstrating the different gene expression profiles in these two groups [18]. In this analysis, we also found that, in AC133 positive AML cells, MPO gene was expressed more in cases without dysplasia than those accompanied with dysplasia (Tsutsumi et al., unpublished data). Since AML/MLD tends to have a worse prognosis than AML/non-MLD [19], the expression of the MPO gene in AC133 positive cells seemed in accordance with the relationship between clinical outcome of AML and the percentage of MPO positive blasts judged by cytochemichal examination of bone marrow smears. These results suggested that the MPO gene would be expressed in an immature fraction of leukemia cells that contains leukemia stem cells, and that the expression level of the MPO gene in AC133 positive cells might be also related to prognosis.

With these backgrounds, we quantitatively measured the expression of the MPO gene in AC133 positive leukemia cells and we found that the level of MPO gene expression divided AML cases into two groups: MPO gene high (MPOg-H) and MPO gene low (MPOg-L).

We confirmed that all AML/MLD cases belonged to MPOg-L. We could also demonstrate the prognosis of MPOg-H group was better than MPOg-L, and that karyotypes related to poor prognosis were found only in MPOg-L. These findings suggested that the level of MPO gene expression in AC133 leukemia cells related to the prognosis of AML.

2. Materials and methods

2.1. Cell separation and purification

After obtaining written informed consent, bone marrow samples were collected from 33 patients with de novo AML before treatment and from 10 healthy volunteers as control.

Table 1
Percentage of AC133 positive cells before and after purification

Case number	Before purification (%)	After purification (%)
7	14	97.4
8	74.5	99.6
9	12.1	98.8
11	63	84.3
14	36.2	99.3
16	65.4	98.8
17	72.4	94.1

The method to purify AC133 positive cells was described previously [18]. Shortly, target cells were selected from bone marrow mononuclear cells with anti-AC133 antibody-conjugated magnetic microbeads and MACS magnetic separation columns (AC133 Isolation Kit, Miltenyi Biotec, Bergisch-Gladbach, Germany).

When the number of AC133 positive cells was more than 1×10^6 after selection (seven cases, Table 1), the percentage of AC133 positive cells was assessed before and after purification using a flowcytometer (FACScan, Becton Dickinson, Oxford, UK) and anti-AC133/2 antibody (Miltenyi Biotec). In other cases, the isolated cells were morphologically examined on cytospin slides (May–Grunwald–Giemsa staining) to check the contamination of promyelocytes.

2.2. Quantitative real-time PCR (RT-PCR)

The expression of the MPO gene was assessed using quantitative real-time PCR method. cDNA was synthesized from total cellular RNA isolated from purified AC133 positive cells (using RNeasy mini, QIAGEN GmbH, Hilden, Germany) with oligo dT primer (ProSTARTM First-strand cDNA Kit, STRATAGENE, CA, USA), that was used as a template for the PCR reaction. RT-PCR was performed using LightCycler, SYBR Green System (Roche Diagnostics, Basel, Switzerland) following the manufacturer's instructions. The PCR was conducted for 40 cycles (95 °C for 15 s, 60 °C for 10 s and 72 °C for 7 s as one cycle) and 45 cycles to amplify the MPO gene and the GAPDH gene, respectively. The sequences of the PCR primer sets were as follows: for MPO gene, 5′-AACTGATGGAGCAGTATGGCACGC-3′ and 5′-TCGCTGCTGCATGCTGAACACACC-3′ and for the GAPDH gene, 5′-GTCAGTGGTGGACCTGACCT-3′ and 5′-TGAGCTTGACAAAGTGGTCG-3′. Data of RT-PCR were standardized with the following control samples: cDNA of the U937 cell line for GAPDH (quantitative range, 10^0 to 10^{-6}) and MPO cDNA for MPO (quantitative range, 10^0 to 10^{-6}). In cases with chromosomal translocation between 8 and 21, AML1-ETO fusion transcript was also quantitatively assessed before and after the purification of AC133 positive fraction (primer sets for the AML1-ETO fusion gene, 5′-CACCTACCACAGAGCCATCAAA-3′ and 5′-ATCCACAGGTGAGTCTGGCATT-3′) [20]. All PCR reactions were performed at least twice. The amplification of target genes were confirmed by examining the melting

curves of products and by the electrophoresis of PCR products on a 2% agarose gel followed by the visualization with ethidium bromide staining.

2.3. Cell staining

In some cases, to show the presence of MPO protein and its enzymatic activity, AC133 positive cells spread on the slides were stained with anti-MPO antibody (Nichirei Corporation, Tokyo, Japan) using a DAKO LSAB + Kit (DAKO Corporation, CA, USA) and with the diaminobdnzidine method [21], respectively. The expression of MPO protein or its enzymatic activity was shown as a percentage of MPO (protein or activity) positive cells.

2.4. Cytogenetic risk group

Based on the karyotype of leukemia cells, patients were classified into either the favorable, intermediate or adverse risk group, defined by the MRC group with minor modification [22,23].

2.5. Statistical analyses

Clinical and hematological data were obtained from the medical record of each case. The comparison of multilineage dysplasia of hematopoietic cells in the presence of leukemia blasts [23] and the presence of Auer body between groups were analyzed using Chi-square test. The cytogenetic risk group was compared using Mantel extension test. WBC count and the percentage of MPO positive blasts among the groups were analyzed using Wilcoxon's rank sum test.

3. Results

3.1. Purification of AC133 positive cells

The percentage of AC133 positive leukemia cells in bone marrow varied from case to case (0.3–76.6% of mononuclear cells in 20 cases tested), and it did not have any relationship to the FAB subtypes of AML (data not shown) as reported previously [24,25]. After purification, an analysis with flowcytometer demonstrated that AC133 was positive in 84.4–99.6% of collected cells (median 98.8%) among seven cases in which we could obtained more than 1×10^6 cells (Table 1). Though the percentages of AC133 positive cells somewhat varied after purification, there was no differentiated myeloid cells, such as promyelocytes, under morphological evaluation of the slides.

Since some of normal stem cells have been shown to have AC133 antigen on its surface, we next assessed whether leukemia cells but not residual normal stem cells were selected by the purification procedure. For this purpose, we utilized cases with a specific chromosomal translocation, t(8;21), and the expression of AML1-ETO fusion gene resulting from this translocation was quantitatively measured after the purification. As shown in Table 2, the expression of AML1-ETO fusion gene was detected in all four cases though its level was distributed from 0.7 to 22.1. It demonstrated that the purified samples contained target leukemia cells in these four cases.

Table 2
Amount of AML1-ETO transcript after selection with AC133 columun

Case number	AML1-ETO/GAPDH ratio
3	7.77
4	22.1
10	0.7
11	4.88
Negative control[a]	<0.01
Kasumi-1 cell line[b]	167.02

[a] M1 case with normal karyptype.
[b] No selection procedure.

3.2. Quantitative measurement of the MPO gene by real-time RT-PCR method

The relative amount of MPO transcript was shown as a ratio of the MPO and GAPDH transcripts (MPO/GAPDH ratio), and the data are summarized in Table 3. Among control samples, the MPO/GAPDH ratio ranged from 3.2 to 11.8, showing similar values. On the other hand, the MPO/GAPDH ratios varied widely in AML cases (0.05–49.9). Referring to the distribution of the ratios among AML samples and that of normal control (Table 3), we divided the AML cases into two groups: MPO gene high group (MPO/GAPDH ratio > 15, MPOg-H, 10 cases) and MPO gene low group (MPO/GAPDH ratio $\leqq$ 15, MPOg-L, 23 cases) so that all normal controls belonged to the MPOg-L group (Fig. 1). In some cases, MPO protein and its enzymatic activity were also examined on the cytospin slides of AC133 positive cells (Table 4). The enzymatic activity of MPO in AC133 positive

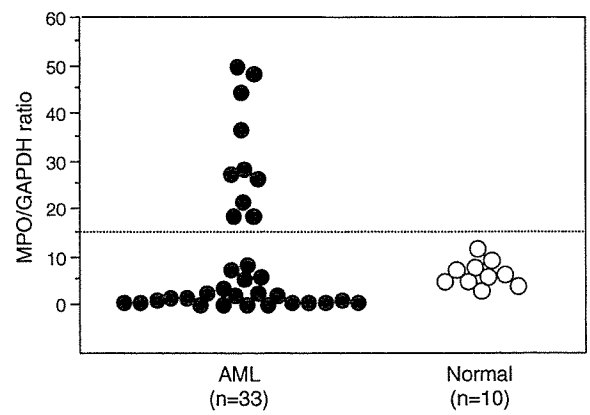

Fig. 1. Relative amount of MPO transcripts in AML cells (33 cases) and normal bone marrow cells (10 cases) selected with AC133-columns. The ratios of the MPO and GAPDH genes are shown as MPO/GAPDH ratio. AML cases were divided into two groups by the ratio (>15 and $\leqq$15). The dotted line shows the ratio, 15.

Table 3
MPO/GAPDH ratio and the percentage of MPO positive blasts

Case number	MPO/GAPDH ratio	BM blast-MPO	FAB	MLD	Cytogenetic risk group	MPOg group
1	7.37	50	M2	+	Adverse, 5q−	L
2	5.37	33	M6	+	Adverse, −5	L
3	44.26	100	M2	−	Favorable, t(8;21)	H
4	36.58	96	M1	−	Favorable, t(8;21)	H
5	0.65	6	M2	+	Adverse, complex	L
6	1.80	45	M2	+	Intermediate, normal	L
7	2.83	35	M2	+	Intermediate, normal	L
8	0.05	2	M0	−	Intermediate, others	L
9	0.07	10	M2	−	Intermediate, normal	L
10	21.46	100	M2	−	Favorable, t(8;21)	H
11	18.77	100	M2	−	Favorable, t(8;21)	H
12	2.35	13	M4	+	Adverse, complex	L
13	0.12	4	M4	−	Intermediate, others	L
14	0.60	3	M6	−	Adverse, complex	L
15	49.91	80	M1	−	Intermediate, normal	H
16	18.67	100	M4	−	Intermediate, others	H
17	8.50	80	M4-Eo	−	Favorable, inv(16)	L
18	0.92	60	M4	+	Intermediate, others	L
19	48.52	98	M2	−	Intermediate, others	H
20	27.55	99	M1	−	Intermediate, normal	H
21	28.34	94	M2	−	Intermediate, others	H
22	2.09	26	M2	+	Intermediate, normal	L
23	0.83	10	M4	−	Intermediate, normal	L
24	2.43	59	M2	+	Adverse, −5	L
25	1.33	2	M0	−	Intermediate, normal	L
26	3.78	80	M2	+	Intermediate, normal	L
27	0.09	5	M4	+	Intermediate, normal	L
28	26.48	100	M1	−	Intermediate, normal	H
29	0.66	84	M2	−	Intermediate, normal	L
30	1.11	45	M2	+	Adverse, complex	L
31	0.53	11	M2	+	Intermediate, normal	L
32	1.58	54	M4	+	ND	L
33	5.95	82	M2	+	Intermediate, normal	L
Normal 1	11.8	ND				
Normal 2	9.5	ND				
Normal 3	8.0	ND				
Normal 4	7.5	ND				
Normal 5	6.5	ND				
Normal 6	6.2	ND				
Normal 7	5.2	ND				
Normal 8	5.0	ND				
Normal 9	4.1	ND				
Normal 10	3.2	ND				

ND, not done; MLD, multilineage dysplasia.

cells was detected mostly in cases belonging to MPOg-H group, and they had high percentages of MPO protein positive cells except for case 33 (Table 4).

We next compared the level of expression of the MPO gene in AC133 positive cells and the percentage of MPO positive leukemia blasts judged on bone marrow slides. The relationship of these two factors is shown in Fig. 2. Cases were classified into the high percentage of MPO (activity) positive blasts (blast MPOa-H group, MPO activity positive blasts > 50%) or the low group (blast MPOa-L group, MPO activity positive blasts $\leqq$ 50%). All cases in the blast MPOa-L group were categorized into MPOg-L (Group III), however, the blast MPOa-H cases comprised of MPOg-H (Group I, 10 cases) and MPOg-L (Group II, 8 cases). It meant that cases in Group II showed high percentage of MPO positive blast on the bone marrow smear but the expression of the MPO gene was low in the AC133 positive fraction. The percentage of MPO positive blasts did not have a statistically significant prognostic impact on overall survival in this series (Fig. 3) but all long-term survivors belonged to the MPOg-H group.

3.3. Clinical characteristics of cases in MPOg-H and MPOg-L groups

Clinical characteristics of AML cases in the MPOg-H and MPOg-L groups are shown in Table 5. There was no statistical difference in age or performance status (PS) among these two groups, however, multilineage morphological dysplasia

Table 4
Percentages of MPO protein or MPO activity positive cells among AC133 purified samples

Case number	MPO/GAPDH ratio	MPOg group	AC133-MPO protein positive cell (%)	AC133-MPO activity positive cell (%)
13	0.12	L	0	0
14	0.60	L	<1	0
17	8.50	L	13	0
18	0.92	L	10	0
19	48.52	H	100	12
20	27.55	H	100	60
21	28.34	H	100	29
23	0.83	L	0	0
24	2.43	L	3	0
25	1.33	L	0	0
26	3.78	L	11	0
28	26.48	H	100	64
31	0.53	L	0	0
32	1.58	L	0	0
33	5.95	L	47	5

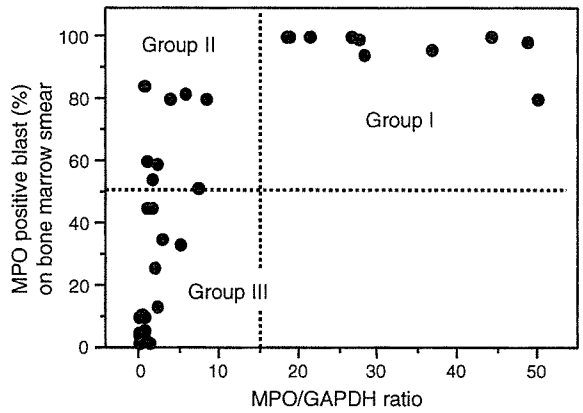

Fig. 2. Relationship between the percentage of MPO positive blasts on bone marrow smear and the amount of the MPO gene in AC133 positive cells. AML cases were categorized into three groups (Groups I–III) by the two factors above. The vertical dotted line shows the MPO/GAPDH ratio, 15, and the horizontal one is for the percentage of MPO positive blasts, 50%. There were 10 cases in Group I, 8 cases in Group II and 15 cases in Group III.

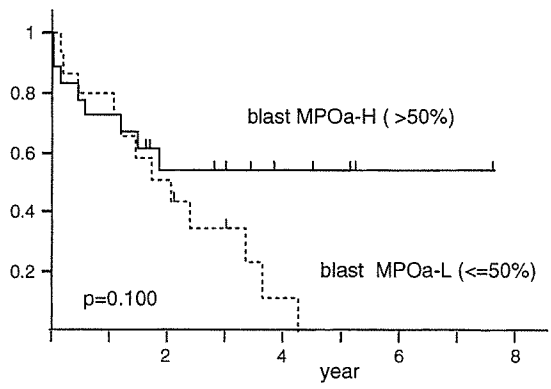

Fig. 3. Overall survival by the percentage of MPO positive blasts on bone marrow smear. There was no statistical significance between the high MPO group (blast MPOa-H) and the low MPO group (blast MPOa-L). The p-value was 0.100.

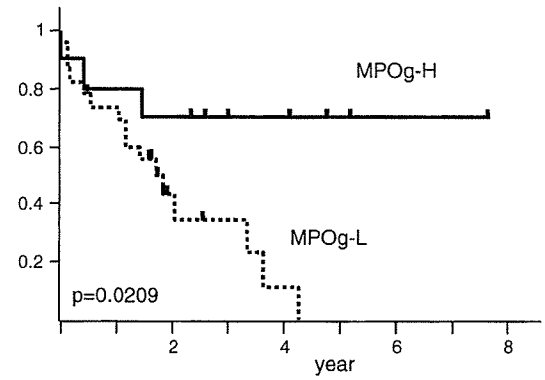

Fig. 4. Overall survival by the amount of MPO gene expression in AC133 positive cells. AML cases with high expression of the MPO gene in AC133 positive cells (MPOg-H) showed better overall survival than those with low expression (MPOg-L) with statistical significance ($p = 0.0209$).

(MLD) in the presence of leukemia blasts was found only in the cases belonging to the MPOg-L group. Distribution of cases in the chromosomal risk groups was also significantly different between MPOg-H and MPOg-L; four out of five cases with favorable karyotypes were in the MPOg-H, and all seven cases with adverse chromosomal risk belonged to the MPOg-L group. Interestingly, although the WBC count at diagnosis was significantly high in the MPOg-H group, overall survival was better in the MPOg-H group than the MPOg-L with statistical significance (Fig. 4).

4. Discussion

Recent reports have demonstrated that AC133 positive bone marrow/cord blood cells are capable of reconstituting long-term hematopoiesis both in mouse and man [12,13,26,27], and that human AML blasts bearing AC133 are able to proliferate and form a leukemic cell population in NOD-SCID mice [11]. From these reports, it has been suggested that normal and malignant hematopoietic stem cells

Table 5
Clinical characteristics of patients in the high and low MPO/GAPDH group

	Total ($n=33$)	High ($n=10$)	Low ($n=23$)	p-Value
Age, Median (range)		34 (27–79)	52 (22–85)	0.0958
PS (0/1/2/3)	5/23/2/3	2/7/1/0	3/16/1/3	0.3445
FAB type				0.0418
M0	2	0	2	
M1	4	4	0	
M2	17	5	12	
M4	8	1	7	
M6	2	0	2	
WBC, median ($\times 10^9\,l^{-1}$)	16.5	58.0	9.9	0.0092
Auer body (present/absent)	14/19	9/1	5/18	0.0003
MPO positivity of blast, median (%)	52	99	34	<0.0001
MLD (present/absent)	15/18	0/10	15/8	0.0005
Cytogenetic risk group				0.0044
Favorable	5	4	1	
Intermediate	20	6	14	
Adverse	7	0	7	
Not done	1	0	1	

MLD, multilineage dysplasia.

were positive for AC133 antigen on the surface. In this study, we measured the amount of MPO transcripts in AC133 positive leukemia cells. As shown in cases with t(8;21), the expression of AML1-ETO fusion transcripts was detectable after positive selection with an AC133-column, demonstrating these four purified samples, at least, contained leukemia cells. Morphological examination showed that the selected cells did not contain any promyelocytes or more mature cells.

The expression of the MPO gene in AML cells was previously reported by several groups [28–30]. Zaki et al. used Northern blot analysis to examine the expression of MPO mRNA in 32 AML samples, and they found that M3 cases had the highest level of expression followed by M2, M4, M1 and M5 cases [28]. Since their results reflected the myeloid differentiation of leukemia cells defined by the FAB subtypes, it seemed that the AML samples they tested (MNC samples, >80% blasts) contained a differentiated fraction of leukemia cells. In our present study, AML with maturation, such as M2 and M4 cases were found in both MPOg-H and MPOg-L groups, showing a clear contrast to the report from Zaki et al. We assume that the amount of MPO mRNA in AC133 positive leukemia cells did not clearly relate to the FAB subgroup of AML defined by the morphological differentiation of leukemia cells.

It has been shown that genes expressed in immature hamatopoietic cells including stem cells do not always represent the lineage commitment [31,32]. Using genetically engineered mice, Ye et al. demonstrated that one of the myeloid specific genes, lysozyme, was expressed in bone marrow cells that have potential to reconstitute both myeloid and lymphoid cells [33]. We do not have any clear answer whether the expression of the MPO gene in AC133 positive leukemia cells was independent of myeloid commitment or it was a part of myeloid differentiation of these cells. The fact that some cells in cases belonging to MPOg-H also expressed MPO protein and its enzymatic activity suggested, at least in these cases, that MPO expression represented the early process of myeloid commitment and/or maturation before apparent morphological differentiation.

Comparing to the MPOg-L, belonging to the MPOg-H group was significantly related to the better survival. Some clinical features repeatedly observed in favorable AML cases were found among cases in the MPOg-H group: all cases with t(8;21) and no cases with adverse karyotypes or MLD were in this group [34]. These data supported the difference in survival between these two groups. We previously demonstrated that the percentage of MPO positive blasts was an independent prognostic factor for AML [8]. However, there was no significant difference in overall survival by the percentage of MPO positive blasts in this study ($p=0.100$), but by the level of the MPO gene in AC133 positive fraction. It might be because of the small number of cases, or it was because the level of the MPO gene in AC133 positive fraction might have a stronger impact on the survival of patients with AML. Survival curve of Group II (high percentage of MPO positive blasts but low MPO/GAPDH ratio) was similar to that of Group III in this series (data not shown). This point needs to be confirmed with a larger number of cases.

In summary, we confirmed that MLD phenotype was significantly related to the low expression of the MPO gene in AC133 positive cells. We also demonstrated the possible prognostic value of the MPOg-H group in overall survival associated with positive relation to the karyotype, t(8;21) and the negative relation to the adverse karyotypes. It is necessary to investigate whether several factors seen in favorable AML cases, such as karyotype and MPO expression have biological relationship at the molecular level.

Acknowledgements

This work was supported in part by grant from the Ministry of Education, Culture, Sports, Science and Technology (Y.M., H.M. and M.T.), and the Ministry of Health, Labour and Welfare of Japan (Y.M.). We thank A. Mizugashira-Kubota and E. Yamazoe for their assistance.

J. Taguchi, Y. Sawayama, K. Ando and C. Tsutsumi worked on the experiments with advices from H. Tsushima. S. Yoshida, T. Fukushima and I. Jinnai collected clinical samples and data, and T. Hata and K. Kuriyama were in charge of the diagnosis. S. Honda performed statistical analyses. Y. Miyazaki organized this project and wrote the paper under the supervision of H. Mano and M. Tomonaga.

References

[1] Babior BM. Oxygen-dependent microbial killing by phagocytes (first of two parts). N Engl J Med 1978;298:659–68.
[2] Babior BM. Oxygen-dependent microbial killing by phagocytes (second of two parts). N Engl J Med 1978;298:721–5.
[3] Koeffler HP, Ranyard J, Pertcheck M. Myeloperoxidase: its structure and expression during myeloid differentiation. Blood 1985;65:484–91.
[4] Winterbourn CC, Vissers MC, Kettle AJ. Myeloperoxidase. Curr Opin Hematol 2000;7:53–8.
[5] Bennett JM, Catovsky D, Daniel MT, Flandrin G, Galton DA, Gralnick HR, et al. Proposed revised criteria for the classification of acute myeloid leukaemia. A report of the French–American–British Cooperative Group. Ann Intern Med 1985;103:620–9.
[6] Hoyle CF, Gray RG, Wheatley K, Swirsky D, de Bastos M, Sherrington P, et al. Prognostic importance of Sudan Black positivity: a study of bone marrow slides from 1386 patients with de novo acute myeloid leukaemia. Br J Haematol 1991;79:398–407.
[7] Matsuo T, Cox C, Bennett JM. Prognostic significance of myeloperoxidase positivity of blast cells in acute myeloblastic leukemia without maturation (FAB: M1): an ECOG study. Hematol Pathol 1989;3:153–8.
[8] Matsuo T, Kuriyama K, Miyazaki Y, Yoshida S, Tomonaga M, Emi N, et al. The percentage of myeloperoxidase-positive blast cells is a strong independent prognostic factor in acute myeloid leukemia, even in the patients with normal karyotype. Leukemia 2003;17:1538–43.
[9] Yin AH, Miraglia S, Zanjani ED, Almeida-Porada G, Ogawa M, Leary AG, et al. AC133, a novel marker for human hematopoietic stem and progenitor cells. Blood 1997;90:5002–12.
[10] Miraglia S, Godfrey W, Yin AH, Atkins K, Warnke R, Holden JT, et al. A novel five-transmembrane hematopoietic stem cell antigen: isolation, characterization, and molecular cloning. Blood 1997;90:5013–21.
[11] Bonnet D, Dick JE. Human acute myeloid leukemia is organized as a hierarchy that originates from a primitive hematopoietic cell. Nat Med 1997;3:730–7.
[12] de Wynter EA, Buck D, Hart C, Heywood R, Coutinho LH, Clayton A, et al. CD34+ AC133+ cells isolated from cord blood are highly enriched in long-term culture-initiating cells, NOD/SCID-repopulating cells and dendritic cell progenitors. Stem Cells 1998;16:387–96.
[13] Bhatia M, Bonnet D, Murdoch B, Gan OI, Dick JE. A newly discovered class of human hematopoietic cells with SCID-repopulating activity. Nat Med 1998;4:1038–45.
[14] Gallacher L, Murdoch B, Wu DM, Karanu FN, Keeney M, Bhatia M. Isolation and characterization of human CD34(−)Lin(−) and CD34(+)Lin(−) hematopoietic stem cells using cell surface markers AC133 and CD7. Blood 2000;95:2813–20.
[15] Shmelkov SV, Jun L, St Clair R, McGarrigie D, Derderian CA, Usenko JK, et al. Alternative promoters regulate transcription of the gene that encodes stem cell surface protein AC133. Blood 2004;103:2055–61.
[16] Ohmine K, Ota J, Ueda M, Ueno S, Yoshida K, Yamashita Y, et al. Characterization of stage progression in chronic myeloid leukemia by DNA microarray with purified hematopoietic stem cells. Oncogene 2001;20:8249–57.
[17] Qian Z, Fernald AA, Godley LA, Larson RA, Le Beau MM. Expression profiling of CD34+ hematopoietic stem/progenitor cells reveals distinct subtypes of therapy-related acute myeloid leukaemia. Proc Natl Acad Sci USA 2002;99:14925–30.
[18] Tsutsumi C, Ueda M, Miyazaki Y, Yamashita Y, Choi YL, Ota J, et al. DNA microarray analysis of dysplastic morphology associated with acute myeloid leukemia. Exp Hematol 2004;32:828–35.
[19] Kuriyama K, Tomonaga M, Matsuo T, Kobayashi T, Miwa H, Shirakawa S, et al., Japan Adult Leukaemia Study Group (JALSG). Poor response to intensive chemotherapy in de novo acute myeloid leukaemia with trilineage myelodysplasia. Br J Haematol 1994;86:767–73.
[20] Gabert J, Beillard E, van der Velden VHJ, Bi W, Grimwade D, Pallisgaard N, et al. Standardization and quality control studies of 'real-time' quantitative reverse transcriptase polymerase chain reaction of fusion gene transcripts for residual disease detection in leukaemia—A Europe Against Cancer Program. Luekemia 2003;17:2318–57.
[21] Shibata A, Bennett JM, Castoldi GL, Catovsky D, Flandrin G, Jaffe ES, et al. Recommended methods for cytological procedures in haematology. International Committee for Standardization in Haematology (ICSH). Clin Lab Haematol 1985;7:55–74.
[22] Grimwade D, Walker H, Oliver F, Wheatley K, Harrison C, Harrison G, et al. The importance of diagnostic cytogenetics on outcome in AML: analysis of 1612 patients entered into the MRC AML 10 trial. The Medical Research Council Adult and Children's Leukaemia Working Parties. Blood 1998;92:2322–33.
[23] Miyazaki Y, Kuriyama K, Miyawaki S, Ohtake S, Sakamaki H, Matsuo T, et al. Cytogenetic heterogeneity of acute myeloid leukaemia (AML) with trilineage dysplasia: Japan Adult Leukaemia Study Group-AML 92 study. Br J Haematol 2003;120:56–62.
[24] Vercauteren SM, Sutherland HJ. CD133 (AC133) expression on AML cells and progenitors. Cytotherapy 2001;3:449–59.
[25] Fauth F, Weidmann E, Martin H, Schneider B, Sonnhoff S, Hoelzer D. AC133 expression on acute myeloid leukemia blasts: correlation to FAB and to CD34 expression and possible implications for peripheral blood progenitor cell purging in AML. Leuk Res 2001;25:191–6.
[26] Kuci S, Wessels JT, Buhring HJ, Schilbach K, Schumm M, Seitz G, et al. Identification of a novel class of human adherent CD34-stem cells that give rise to SCID-repopulating cells. Blood 2003;101:869–76.
[27] Koehl U, Zimmermann S, Esser R, Sorensen J, Gruttner HP, Duchscherer M, et al. Autologous transplantation of CD133 selected hematopoietic progenitor cells in a pediatric patient with relapsed leukemia. Bone Marrow Transplant 2002;29:927–30.
[28] Zaki SR, Austin GE, Swan D, Srinivasan A, Ragab AH, Chan WC. Human myeloperoxidase gene expression in acute leukemia. Blood 1989;74:2096–102.
[29] Chang KS, Trujillo JM, Cook RG, Stass SA. Human myeloperoxidase gene: molecular cloning and expression in leukemic cells. Blood 1986;68:1411–4.
[30] Austin GE, Chan WC, Zhao W, Racine M. Myeloperoxidase gene expression in normal granulopoiesis and acute leukemias. Leuk Lymphoma 1994;15:209–20.
[31] Hu M, Krause D, Greaves M, Sharkis S, Dexter M, Heyworth C, et al. Multilineage gene expression precedes commitment in the hemopoietic system. Genes Dev 1997;11:774–85.

[32] Akashi K, Traver D, Miyamoto T, Weissman IL. A clonogenic common myeloid progenitor that gives rise to all myeloid lineages. Nature 2000;404:193–7.
[33] Ye M, Iwasaki H, Laiosa CV, Stadtfeld M, Xie H, Heck S, et al. Hematopoietic stem cells expressing the myeloid lysozyme gene retain long-term, multilineage repopulation potential. Immunity 2003;19:689–99.
[34] Lowenberg B, Downing JR, Burnett A. Acute myeloid leukemia. N Engl J Med 1999;341:1051–62.

Oncogene (2006) 25, 139–146

www.nature.com/onc

SHORT COMMUNICATION

Epigenetic silencing of *AXIN2* in colorectal carcinoma with microsatellite instability

K Koinuma[1,2], Y Yamashita[1], W Liu[3], H Hatanaka[1], K Kurashina[1,2], T Wada[1], S Takada[1], R Kaneda[1], YL Choi[1], S-I Fujiwara[1], Y Miyakura[2], H Nagai[2] and H Mano[1,4]

[1]*Division of Functional Genomics, Jichi Medical School, Tochigi, Japan;* [2]*Department of Surgery, Jichi Medical School, Tochigi, Japan;* [3]*Division of Experimental Pathology, Mayo Clinic and Mayo Medical School, Rochester, MN, USA and* [4]*CREST, Japan Science and Technology Agency, Saitama, Japan*

Mutation or epigenetic silencing of mismatch repair genes, such as *MLH1* and *MSH2*, results in microsatellite instability (MSI) in the genome of a subset of colorectal carcinomas (CRCs). However, little is yet known of genes that directly contribute to tumor formation in such cancers. To characterize MSI-dependent changes in gene expression, we have now compared transcriptomes between fresh CRC specimens positive or negative for MSI ($n = 10$ for each) with the use of high-density oligonucleotide microarrays harboring >44 000 probe sets. Correspondence analysis of the expression patterns of isolated MSI-associated genes revealed that the transcriptome of MSI$^+$ CRCs is clearly distinct from that of MSI$^-$ CRCs. Such MSI-associated genes included that for AXIN2, an important component of the WNT signaling pathway. *AXIN2* was silenced, apparently as a result of extensive methylation of its promoter region, specifically in MSI$^+$ CRC specimens. Forced expression of *AXIN2*, either by treatment with 5′-azacytidine or by transfection with *AXIN2* cDNA, resulted in rapid cell death in an MSI$^+$ CRC cell line. These data indicate that epigenetic silencing of *AXIN2* is specifically associated with carcinogenesis in MSI$^+$ CRCs.

Oncogene (2006) **25,** 139–146. doi:10.1038/sj.onc.1209009; published online 10 October 2005

Keywords: epigenetics; colorectal carcinoma; microsatellite instability; AXIN2; MLH1

Colorectal carcinoma (CRC) is one of the leading causes of cancer death in humans. Evidence indicates the existence of two major types of genomic instability in CRCs: chromosomal instability and microsatellite instability (MSI) (Lengauer *et al.*, 1998). Whereas chromosomal instability is associated with an abnormal DNA content (such as aneuploidy), inactivation of the tumor suppressor gene *TP53*, and activation of oncogenes (Kinzler and Vogelstein, 1996), MSI is associated with defects in DNA mismatch repair (MMR) that result in frameshift mutations in microsatellite repeats and thereby affect the structure of genes containing such repeats (Ionov *et al.*, 1993).

Although germline mutations of MMR genes have been detected in the genome of individuals with hereditary nonpolyposis colorectal cancer (Fishel *et al.*, 1993; Bronner *et al.*, 1994; Papadopoulos *et al.*, 1994), many sporadic CRCs positive for MSI are associated with epigenetic silencing of nonmutated MMR genes (Toyota *et al.*, 1999; Miyakura *et al.*, 2001). MSI$^+$ CRCs are characterized by specific clinicopathologic features and gene mutations. They occur with a higher frequency in women than in men, develop in the right side of the colon, and manifest a mucinous or poorly differentiated histopathology. Many of the CpG dinucleotides within the promoter region of the MMR gene *MLH1* are methylated (Cunningham *et al.*, 1998; Veigl *et al.*, 1998) and the *BRAF* gene frequently contains activating mutations (Koinuma *et al.*, 2004) in MSI$^+$ CRCs. Multiple genomic fragments have been found to be methylated in such CRCs (Toyota *et al.*, 1999), and an entity of CRC with a CpG island methylator phenotype has been proposed (Issa, 2004). The repertoire of genes that become methylated specifically in CRCs positive for *MLH1* methylation has remained uncharacterized, however.

To characterize directly the transcriptome specifically associated with MSI$^+$ CRC, we have now compared transcriptomes between fresh CRC specimens with or without MSI. Unexpectedly, we found that the expression of *AXIN2*, which encodes a component of the WNT signaling pathway, was markedly suppressed among the former tumors. CpG sequences within the *AXIN2* promoter were revealed to be extensively methylated in such CRCs. Forced expression of *AXIN2* inhibited cell proliferation in an MSI$^+$ CRC cell line, indicating that loss of *AXIN2* transcription is directly associated with carcinogenesis in MSI$^+$ CRCs.

To identify genes whose expression is specifically altered in MSI$^+$ CRCs, we first compared the transcriptomes of CRCs with or without MSI. A total of 248 consecutive cases of CRC were examined for MSI status

Correspondence: Professor H Mano, Division of Functional Genomics, Jichi Medical School, 3311-1 Yakushiji, Kawachigun, Tochigi 329-0498, Japan.
E-mail: hmano@jichi.ac.jp
Received 28 April 2005; revised 7 July 2005; accepted 13 July 2005; published online 10 October 2005

as well as for methylation of the promoter region of *MLH1* (Koinuma *et al.*, 2004). Most ($n=213$) of the cancer specimens were MSI$^-$, with the remainder ($n=35$) being positive for MSI. To compare the transcriptomes of these two subtypes of CRC, we randomly selected 10 specimens from each group and subjected them to gene expression profiling with microarrays (Affymetrix GeneChip HGU133) that harbor >44 000 probe sets. The clinical characteristics of the patients whose CRC specimens were subjected to microarray analysis are summarized in Table 1.

To exclude transcriptionally silent genes from our analyses, we first chose probe sets that received the 'Present' call from Microarray Suite 5.0 (Affymetrix) in at least 10% ($n=2$) of the samples. Two-way hierarchical clustering (Alon *et al.*, 1999) of the 20 patients based on the expression profiles of the isolated 21 888 probe sets failed to separate those with MSI$^+$ CRC from those with MSI$^-$ CRC (data not shown). We therefore attempted to identify 'MSI-associated probe sets' whose expression intensities differed significantly (Student's *t*-test, $P<0.001$) between the two classes and whose effect size (absolute difference in mean expression level) was $\geqslant 50$ U. Two-way clustering analysis with the 24 probe sets that fulfilled both these criteria clearly separated the individuals of the two clinical classes (Figure 1a). The distinct transcriptomes of the two classes were also confirmed by correspondence analysis (Fellenberg *et al.*, 2001), which reduced the complexity of the gene expression patterns from 24 to three dimensions. Projection of the study subjects into a virtual three-dimensional space based on their calculated coordinates revealed that the MSI$^+$ specimens were positioned apart from the MSI$^-$ ones (Figure 1b). These data indicate that the two classes of CRC possess distinct gene expression profiles, or 'molecular signatures', and they also suggest the feasibility of gene expression-based differential diagnosis of the two CRC subtypes.

Table 1 Clinical characteristics of the study subjects enrolled in microarray analysis

Patient ID	*Age (years)*	*Sex*	*MSI status*	MLH1 *methylation*	BRAF *gene*	KRAS2 *gene*	*Tumor site*	*Dukes stage*	*Pathology*	AXIN2 *methylation*
225	83	Female	Positive	Yes	Mutant	Wild	Proximal	C	Well	Yes
263	86	Female	Positive	Yes	Mutant	Wild	Proximal	C	Mod	Yes
280	83	Female	Positive	Yes	Mutant	Wild	Proximal	C	Well	Yes
305	74	Male	Positive	Yes	Mutant	Wild	Proximal	B	Sig	No
318	76	Female	Positive	Yes	Mutant	Wild	Proximal	B	Well	Yes
336	68	Male	Positive	Yes	Mutant	Wild	Proximal	B	Muc	No
413	69	Female	Positive	Yes	Mutant	Wild	Proximal	A	Well	No
416	76	Female	Positive	Yes	Mutant	Wild	Proximal	B	Muc	No
433	54	Female	Positive	Yes	Wild	Wild	Proximal	D	Well	Yes
479	74	Female	Positive	Yes	Mutant	Wild	Proximal	B	Mod	No
238	74	Male	Negative	No	Wild	Mutant	Distal	A	Well	No
249	62	Male	Negative	No	Wild	Wild	Proximal	B	Well	No
278	73	Male	Negative	No	Wild	Wild	Proximal	C	Well	No
295	71	Female	Negative	No	Wild	Mutant	Proximal	C	Well	No
298	70	Male	Negative	No	Wild	Mutant	Proximal	D	Well	No
307	80	Female	Negative	No	Wild	Wild	Proximal	C	Mod	No
308	62	Male	Negative	No	Wild	Wild	Distal	B	Mod	No
319	53	Female	Negative	No	Wild	Wild	Distal	A	Well	No
419	45	Female	Negative	No	Wild	Mutant	Proximal	D	Muc	No
426	42	Female	Negative	No	Wild	Wild	Proximal	C	Well	No

Well = well-differentiated adenocarcinoma; Mod = moderately differentiated adenocarcinoma; Sig = signet ring cell adenocarcinoma; Muc = mucinous adenocarcinoma. Methylation of *AXIN2* promoter region was determined by COBRA method.

Figure 1 Comparison of transcriptomes between CRCs positive or negative for MSI. (**a**) Subject tree generated by two-way clustering analysis with 24 probe sets that contrasted the two clinical conditions ($P<0.001$; effect size, $\geqslant 50$ U). Tumor samples were obtained from individuals with sporadic CRC who underwent surgical treatment at Jichi Medical School Hospital. Written informed consent was obtained from all patients, and the present study was approved by the ethics committee of Jichi Medical School. Microsatellite stability was determined by analysis of nine microsatellite repeat loci (three dinucleotide repeats and six mononucleotide repeats) as described previously (Miyakura *et al.*, 2001), and MSI status was stratified according to the criteria of the National Cancer Institute workshop (Boland *et al.*, 1998). Total RNA was extracted from ~100 mg of tissue, and was used in the hybridization experiments with GeneChip HGU133 A&B microarrays (Affymetrix), which harbor >44 000 probe sets corresponding to ~33 000 human genes, as described previously (Ohki-Kaneda *et al.*, 2004). The mean expression intensity of the internal positive control probe sets (http://www.affymetrix.com/support/technical/mask_files.affx) on the microarrays was set to 500 units (U) in each hybridization, and the fluorescence intensity of each probe set was normalized accordingly. All normalized array data are available at the Gene Expression Omnibus website (http://www.ncbi.nlm.nih.gov/geo) under the Accession Number GSE2138. Each column corresponds to a separate sample (MSI$^-$, green; MSI$^+$, red), and each row to a probe set whose expression is color-coded according to the indicated scale. Gene symbols are shown on the right; 225541_at, 226545_at, and 242414_at are expressed sequence tag IDs designated by Affymetrix (http://www.affymetrix.com). Annotations and expression intensities for the probe sets are presented in Supplementary Table 1. Note that *MLH1* expression was specifically suppressed in the MSI$^+$ samples. (**b**) Samples were projected into a virtual space with coordinates calculated by correspondence analysis of the 24 probe sets shown in (**a**). Correspondence analysis was performed with ViSta software (http://www.visualstats.org) for all genes showing a significant difference.

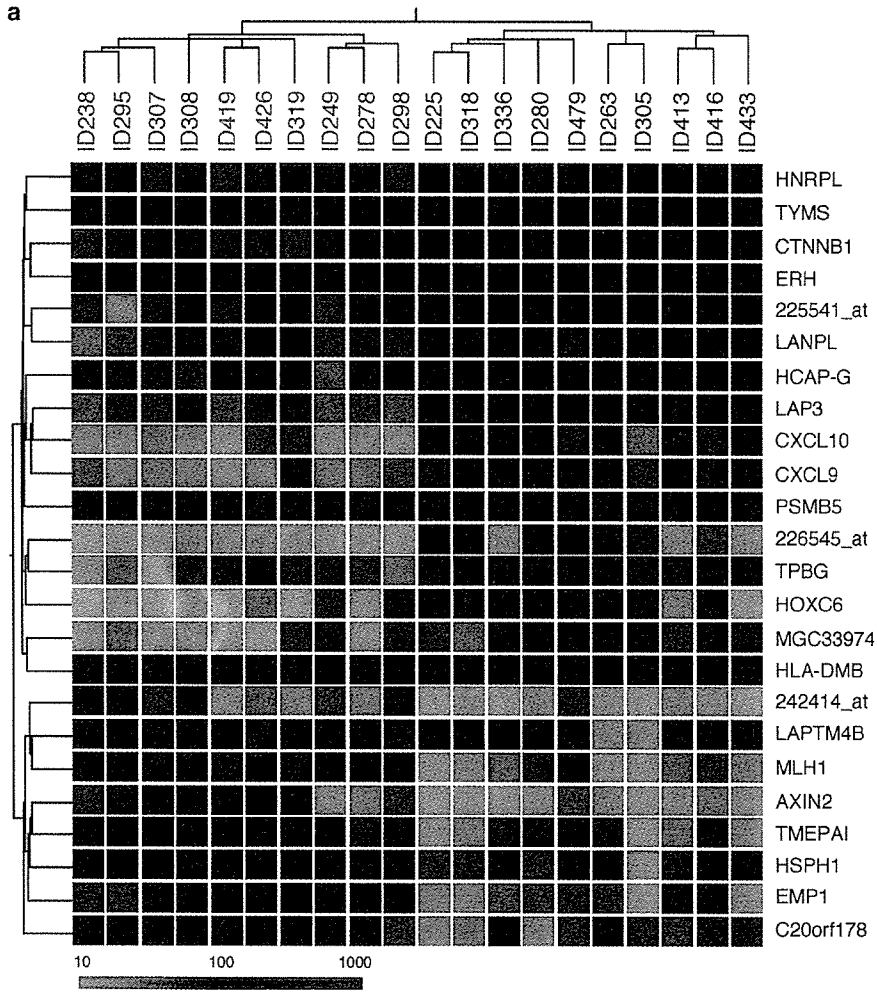
a
ID238
ID295
ID307
ID308
ID419
ID426
ID319
ID249
ID278
ID298
ID225
ID318
ID336
ID280
ID479
ID263
ID305
ID413
ID416
ID433
HNRPL
TYMS
CTNNB1
ERH
225541_at
LANPL
HCAP-G
LAP3
CXCL10
CXCL9
PSMB5
226545_at
TPBG
HOXC6
MGC33974
HLA-DMB
242414_at
LAPTM4B
MLH1
AXIN2
TMEPAI
HSPH1
EMP1
C20orf178
10
100
1000
b
1st dimension
2nd dimension
3rd dimension
MSI-positive
MSI-negative

The isolated MSI-associated genes include *AXIN2* and *CTNNB1* (β-catenin), both of which encode key participants in the WNT signaling pathway (Tolwinski and Wieschaus, 2004). Dysregulation of ubiquitin-dependent degradation of β-catenin contributes to carcinogenesis in a variety of CRCs and hepatocellular carcinomas (Narayan and Roy, 2003). AXIN2, similar to AXIN1, functions as a scaffold protein to facilitate this ubiquitination process by recruiting adenomatous polyposis coli (APC), glycogen synthase kinase-3β, and β-catenin (Behrens *et al.*, 1998). Defects in the degradation of β-catenin have been shown to result from mutations in *AXIN1*, *AXIN2*, *APC*, or *CTNNB1* (Rubinfeld *et al.*, 1997; Liu *et al.*, 2000; Satoh *et al.*, 2000; Smith *et al.*, 2002). Our data therefore suggest that transcriptional suppression of *AXIN2* might represent a novel mechanism by which the function of the APC-AXIN–β-catenin complex is impaired in CRC.

To confirm the MSI-associated change in *AXIN2* expression, we measured the abundance of the corresponding mRNA in the original 20 study specimens by quantitative reverse transcription–polymerase chain reaction (RT–PCR) analysis (Figure 2a). Comparison of the amount of *AXIN2* mRNA determined by RT–PCR with that determined by microarray analysis yielded a Pearson's correlation coefficient (r) of 0.89, indicating that the two data sets were highly correlated ($P<0.001$). (Also see Supplementary Figure 1 for verification of microarray data by RT–PCR.)

With the use of RT–PCR, we then measured the amount of *AXIN2* mRNA in a larger number of samples (seven additional specimens of MSI^+ CRC, for a total of 17; 10 additional specimens of MSI^- CRC, for a total of 20; three MSI^+ CRC cell lines; two MSI^- CRC cell lines). The abundance of *AXIN2* transcripts in most of the MSI^+ CRC specimens and cell lines was reduced compared with that in the MSI^- ones (Figure 2b); an *AXIN2*/*ACTB* transcript ratio of $<5\times10^{-4}$ was apparent in 13 of the 17 MSI^+ CRC specimens, but in only five of the 20 MSI^- ones (Fisher's exact probability test, $P=0.003$). Importantly, a similar MSI-dependent suppression of *AXIN1* expression was not observed among these specimens ($P=0.31$) (data not shown).

Human *AXIN2* possesses a relatively large CpG island within its promoter region (nucleotide positions, chr17: 60986365–60987824). We therefore examined the methylation status of the CpG sites within this region by nucleotide sequencing after sodium bisulfite treatment. Extensive methylation of the CpG island in the *AXIN2* promoter was apparent in CRC specimens positive for MSI and for the loss of *AXIN2* expression (Figure 2c). The promoter region in the MSI^+ CRC cell line HCT116 (Wheeler *et al.*, 1999) was also heavily methylated. The *MLH1* promoter in HCT116 cells is not methylated, but the coding sequence of the gene contains a mutation that results in MSI (Wheeler *et al.*, 1999).

On the basis of these findings, we examined the methylation status of the *AXIN2* promoter in 37 clinical specimens and five cell lines by combined bisulfite restriction analysis (COBRA) (Xiong and Laird, 1997). CpG methylation was detected in five of the 17 MSI^+ specimens, but in none of the 20 MSI^- specimens (Table 1; see Supplementary Table 2). Methylation of the *AXIN2* promoter was not detected in normal colon tissue obtained from the individuals with MSI^+ CRC (data not shown), suggesting that *AXIN2* methylation was a somatic event in these patients.

We then tested whether the amount of the encoded protein correlated with that of *AXIN2* mRNA in CRC specimens (Figure 2d). Immunohistochemical staining showed that AXIN2 was abundant in a specimen with a high mRNA content (ID308), but was present in much smaller amounts in two specimens with a low mRNA content (ID263, ID295). Although a large amount of *AXIN2* mRNA was not always associated with a large amount of protein, a small amount of mRNA was consistently associated with a small amount of protein (data not shown).

To examine directly whether epigenetic silencing of *AXIN2* is relevant to the change in the growth properties of CRC cells, we restored *AXIN2* expression, either by 5′-azacytidine treatment or by introduction of *AXIN2* cDNA, in an MSI^+ CRC cell line. 5′-Azacytidine inhibits *de novo* methylation of genomic DNA and thereby induces demethylation of the genome of proliferating cells (Christman, 2002). HCT116 cells were incubated for 3 days with various concentrations of 5′-azacytidine and were then subjected to COBRA for determination of the methylation status of the *AXIN2* promoter. Treatment with 5′-azacytidine reduced the level of methylation of the *AXIN2* promoter in a concentration-dependent manner (Figure 3a). This effect of 5′-azacytidine was accompanied by an increase in the amount of *AXIN2* mRNA in the cells (Figure 3b) as well as by the induction of cell death (Figure 3c).

Given that 5′-azacytidine likely affects the transcription of other genes in addition to that of *AXIN2*, the growth inhibitory effect observed in HCT116 cells might not have been attributable solely to the induction of *AXIN2* expression. To examine the direct effect of *AXIN2*, we introduced its cDNA into HCT116 cells by transfection. However, an introduction of *AXIN2* cDNA (even with the use of an inducible system) resulted in rapid cell death, and we could not establish stable transformants of cell lines with such expression constructs (data not shown). Therefore, we generated an amphotropic recombinant retrovirus that confers simultaneous expression of both an MYC epitope-tagged form of AXIN2 and mouse CD8. Human kidney 293 cells infected with this virus, but not those infected with a mock virus, expressed AXIN2 (Figure 3d). HCT116 cells were then infected with the virus and were subjected to affinity chromatography 48 h thereafter to isolate cells that express CD8. Given that CD8-expressing cells would be expected also to express AXIN2, this column purification step should result in rapid enrichment of AXIN2-expressing cells. The isolated cells indeed contained a substantial amount of *AXIN2* mRNA as revealed by RT–PCR (Figure 3e). The purified $CD8^+$ HCT116 cells were then cultured for 3 days to characterize their growth properties. Forced expression of AXIN2 resulted in marked inhibition of cell growth

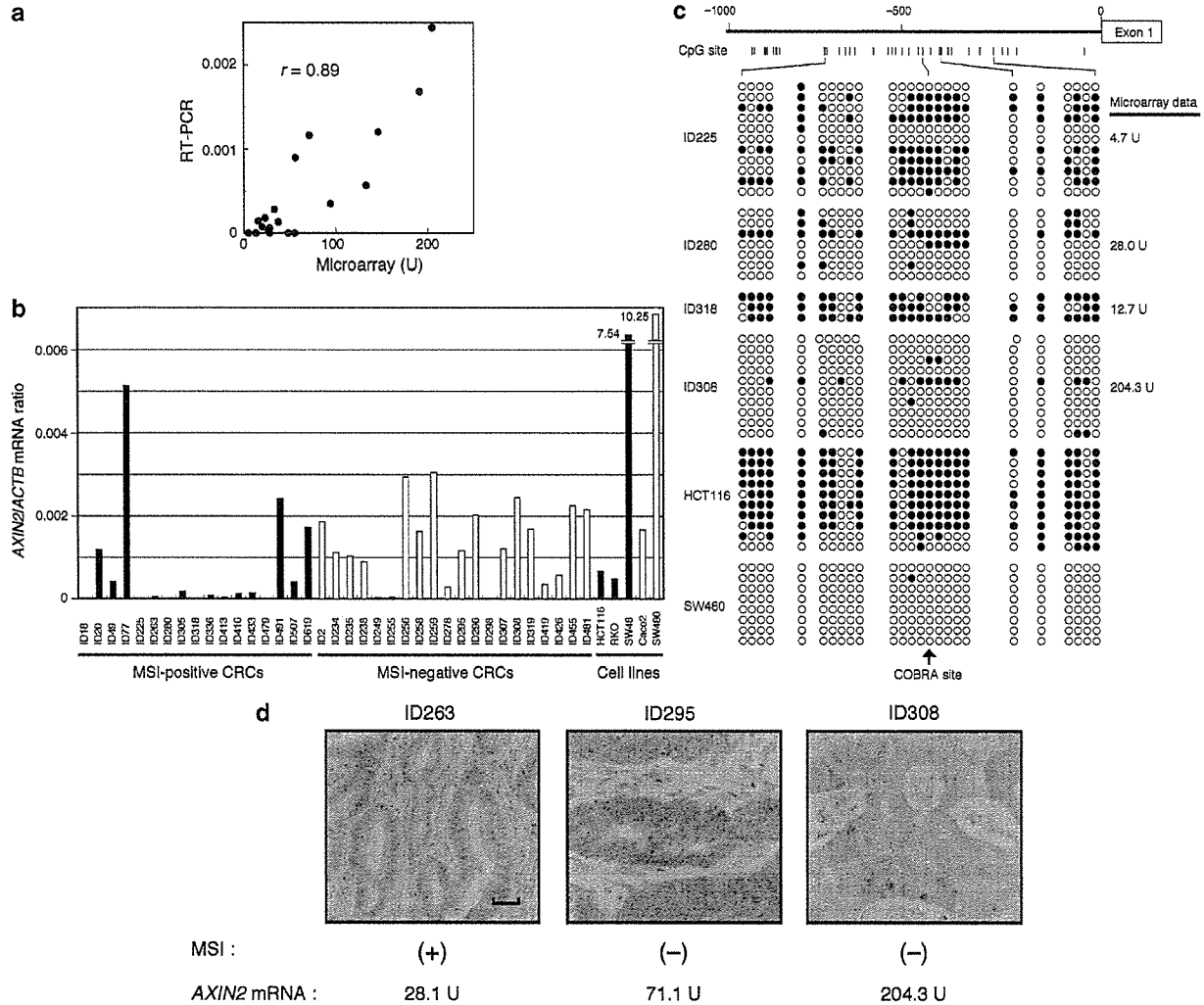

Figure 2 Suppression of *AXIN2* expression in CRCs positive for MSI. (**a**) Comparison of the abundance of *AXIN2* mRNA in study specimens as determined by microarray and RT–PCR analyses. For the latter, the amount of *AXIN2* mRNA was expressed relative to that of *ACTB* mRNA. Pearson's correlation coefficient (*r*) for the comparison is indicated. Portions of double-stranded cDNA were subjected to PCR with a QuantiTect SYBR Green PCR Kit (Qiagen). The amplification protocol comprised incubations at 94°C for 15 s, 63°C for 30 s, and 72°C for 60 s. Incorporation of the SYBR Green dye into PCR products was monitored in real time with an ABI PRISM 7700 sequence detection system (PE Applied Biosystems), thereby allowing determination of the threshold cycle (C_T) at which exponential amplification of products begins. The amount of target cDNAs relative to that of the β-actin (*ACTB*) cDNA was calculated from the C_T values with the use of Sequence Detector ver. 1.6.3 software (PE Applied Biosystems). The primers used for PCR amplification were 5′-CTGGCTCCAGAAGATCACAAAG-3′ and 5′-ATCTCCTCAAACACCGCTCCA-3′ for *AXIN2* and 5′-CCATCATGAAGTGTGACGTGG-3′ and 5′-GTCCGCCTAGAAGCATTTGCG-3′ for *ACTB*. (**b**) Comparison of the amount of *AXIN2* mRNA relative to that of *ACTB* mRNA (as determined by RT–PCR) between MSI$^+$ (closed bars) and MSI$^-$ (open bars) CRC specimens and cell lines. (**c**) Genomic DNA of the indicated clinical specimens and CRC cell lines was treated with sodium bisulfite (Koinuma *et al*., 2004), after which the *AXIN2* promoter region was amplified by PCR with the primers 5′-TTGTATATAGTTTA GYGGTTGGG-3′ and 5′-AAATCTAAACTCCCTACACACTT-3′. Closed and open circles indicate methylated and unmethylated CpG sites, respectively. The positions of the CpG sites are indicated at the top, the *Hha*I digestion site for COBRA is indicated by the arrow, and the microarray data for *AXIN2* expression are shown on the right. (**d**) Immunohistochemical analysis of the indicated clinical specimens with antibodies to AXIN2. The MSI status and the expression level of *AXIN2* determined by microarray analysis are indicated. Immunohistochemical analysis of AXIN2 expression was performed as described previously (Leung *et al*., 2002). Sections (5 μm) of formalin-fixed, paraffin-embedded tissue were mounted on Probe-On slides (Fisher Scientific), which were then incubated first for 1 h at room temperature with 1.5% normal horse serum and then overnight at 4°C with goat polyclonal antibodies to AXIN2 (Santa Cruz Biotechnology). Immune complexes were detected by the avidin–biotin–peroxidase method with 3,3′-diaminobenzidine as the chromogenic substrate (Vectastain ABC kit, Vector Laboratories). The sections were counterstained with hematoxylin. Scale bar, 50 μm.

(Figure 3f), indicating that silencing of *AXIN2* is indeed relevant to tumorigenesis. We also examined if the expression of *AXIN2* directly suppresses the WNT signaling pathway. For this purpose, we utilized a luciferase-based reporter plasmid (TOPflash) for the T-cell factor (TCF) activity, which is a direct target of

β-catenin (Korinek *et al.*, 1997). As shown in Figure 3g, a forced expression of *AXIN2* induced a marked suppression in the luciferase activity in HCT116 cells. On the other hand, *AXIN2* did not affect luciferase activity driven by a mutated, nonfunctional TCF-binding sites (FOPflash). These data clearly indicate that AXIN2 is involved in the WNT–APC–β-catenin pathway in CRCs.

We have demonstrated preferential transcriptional silencing of *AXIN2* in MSI$^+$ CRCs. Recently, mutations within exon 7 of the *AXIN2* gene have been reported in MSI$^+$ CRC specimens (Liu *et al.*, 2000; Wu *et al.*, 2001). We have thus analysed the nucleotide sequence of the *AXIN2* gene among our MSI$^+$ samples ($n=9$). Sequencing of the *AXIN2* exon 7 has revealed that only one patient (ID no. 263) carried a mutated *AXIN2* gene in one allele (data not shown). A deletion of a cytosine residue at the nucleotide position 2096 of the *AXIN2* cDNA (GenBank Accession Number, AF078165) led to a frame shift in the open-reading frame in this patient, introducing a premature termination codon in AXIN2 protein at the amino-acid position of 688. However, majority of the patients had intact *AXIN2* genes, indicating that silencing, but not mutation, of *AXIN2* is the main pathway to impede the *AXIN2* function.

The COBRA experiments revealed that the promoter region of *AXIN2* was extensively methylated in MSI$^+$ CRCs but not in MSI$^-$ CRCs. Although the difference in the frequency of *AXIN2* methylation between these two classes of tumor was significant (Fisher's exact probability test, $P=0.003$), the frequency for the MSI$^+$ specimens was still only 29% and therefore was not able to account for all the observed instances of suppression of *AXIN2* expression. We judged COBRA data as positive for methylation if $\geqslant 10\%$ of the PCR products were digested by *Hha*I. However, a small proportion ($<10\%$) of the PCR products was digested in the analysis of ~50% of MSI$^+$ CRC specimens (data not shown), indicating that alterations in the methylation status of the *AXIN2* promoter were more widespread. It is therefore possible that CpG sites other than that targeted by COBRA are more frequently methylated in MSI$^+$ CRCs and are more important for transcriptional regulation.

Similar promoter methylation has been recently described for other genes important for the WNT signaling pathway. The genes for secreted frizzled-related proteins are thus epigenetically silenced in MSI$^+$ CRCs, resulting in constitutive activation of the WNT pathway (Suzuki *et al.*, 2004). CpG sites within the *APC* promoter were also found to be frequently methylated in CRCs and other cancers (Esteller *et al.*, 2000; Zysman *et al.*, 2002). These data thus suggest that not only genetic mutations but also epigenetic silencing might play an important role in tumorigenesis mediated by activation of the WNT pathway.

Methylation of the *APC* promoter in endometrial cancer has been shown to occur preferentially in MSI$^+$ tumors (Zysman *et al.*, 2002). Despite the lack of an MSI-associated difference in the expression of *APC* in our CRC specimens (data not shown), the results of this previous study together with our present findings suggest the possibility that genes related to the WNT signaling pathway are targeted for methylation specifically in cancers with MSI. Our data further indicate that such methylation in MSI$^+$ cancers may be directly relevant to the mechanism of malignant transformation through epigenetic silencing of tumor suppressor genes. MSI$^+$ CRCs have been thought to arise through genetic events distinct from those that underlie MSI$^-$ cancers (Rajagopalan and Lengauer, 2004), which are frequently associated with aneuploidy and mutations in WNT pathway genes such as *APC* and *CTNNB1*. However, our data indicate that the molecular mechanisms for malignant transformation overlap between MSI$^+$ and MSI$^-$ CRCs.

Figure 3 Induction of cell death by restoration of *AXIN2* expression in a CRC cell line with a methylated *AXIN2* promoter. (**a**) HCT116 cells were incubated for 72 h with 0, 0.2, or 1 μM 5′-azacytidine and were then subjected to COBRA for determination of the methylation status of the *AXIN2* promoter (Xiong and Laird, 1997). Genomic DNA was denatured, incubated for 16 h at 55°C in 3.1 M sodium bisulfite, and then subjected to PCR with the primers in Figure 2c. The PCR products were then digested with the restriction endonuclease *Hha*I (Takara Bio), and the resulting DNA fragments were fractionated by polyacrylamide gel electrophoresis. The gel was stained with SYBR Green I (Takara Bio) and scanned with an LAS3000 imaging system (Fuji Film). Genomic fragments were determined to be positive for CpG methylation if $\geqslant 10\%$ of the PCR products were cleaved by the restriction endonuclease. Lane M, DNA size markers (50-bp ladder). (**b**) The cells from (**a**) were also subjected to RT–PCR analysis for determination of the amount of *AXIN2* mRNA relative to that of *ACTB* mRNA. (**c**) Cells treated as in (**a**) with 0, 0.2, 1, or 5 μM 5′-azacytidine were examined by light microscopy. Cell death was estimated by counting the remaining viable cells in each culture dish by the dye-exclusion method. Scale bar, 50 μm. (**d**) Human kidney 293 cells infected with either a mock virus or a recombinant virus encoding both MYC epitope-tagged AXIN2 and mouse CD8. A human cDNA for AXIN2 tagged at its NH_2-terminus with the MYC epitope sequence was ligated into the pMX-iresCD8 retroviral plasmid (Yamashita *et al.*, 2001) to yield pMX-AXIN2-MYC-iresCD8. The latter plasmid was introduced into BOSC23 cells together with pE-ampho and pGP packaging plasmids (Takara Bio) by transfection with the use of Lipofectamine (Invitrogen). The culture supernatant containing recombinant viruses was added to 293 cells with 4 μg/ml of polybrene (Sigma). Cells were then subjected to immunoprecipitation with the antibodies to MYC (9E10, Roche Diagnostics), and to immunoblot analysis with the same antibodies. (**e**) HCT116 cells infected with the viruses in (**d**) were subjected to affinity chromatography to isolate CD8$^+$ cells, which were then subjected to RT–PCR analysis for quantitation of *AXIN2* mRNA relative to the amount of *ACTB* mRNA. (**f**) The CD8$^+$ fractions in (**e**) were seeded at a density of 5×10^4 cells/dish and cultured for 72 h, after which the ratio of the final cell number to the initial value was determined. Data are means + s.d. of triplicate from a representative experiment. The *P*-value for the indicated comparison was determined by Student's *t* test. (**g**) HCT116 cells were seeded at a density of 2.5×10^6 cells/6 cm dish. After 24 h of incubation, the cells were transfected, with the use of Lipofectamine, with 2 μg of pMX-AXIN2-MYC-iresCD8 (AXIN2) or pMX-iresCD8 (Mock). For the reporter plasmids, 0.5 μg of pGL4 (Promega, Madison, WI, USA) plus either 0.5 μg of pTOPflash or 0.5 μg of pFOPflash (both from Upstate Biotechnology, Lake Placid, NY, USA) were added to the lipofection mix. The activity of *Photinus pyralis* luciferase was measured after 24 h of incubation with the use of the Dual-luciferase reporter assay system (Promega), and normalized on the basis of the activity of *Renilla reniformis* luciferase produced by pGL4. Data are shown as the mean value + s.d. of triplicate samples.

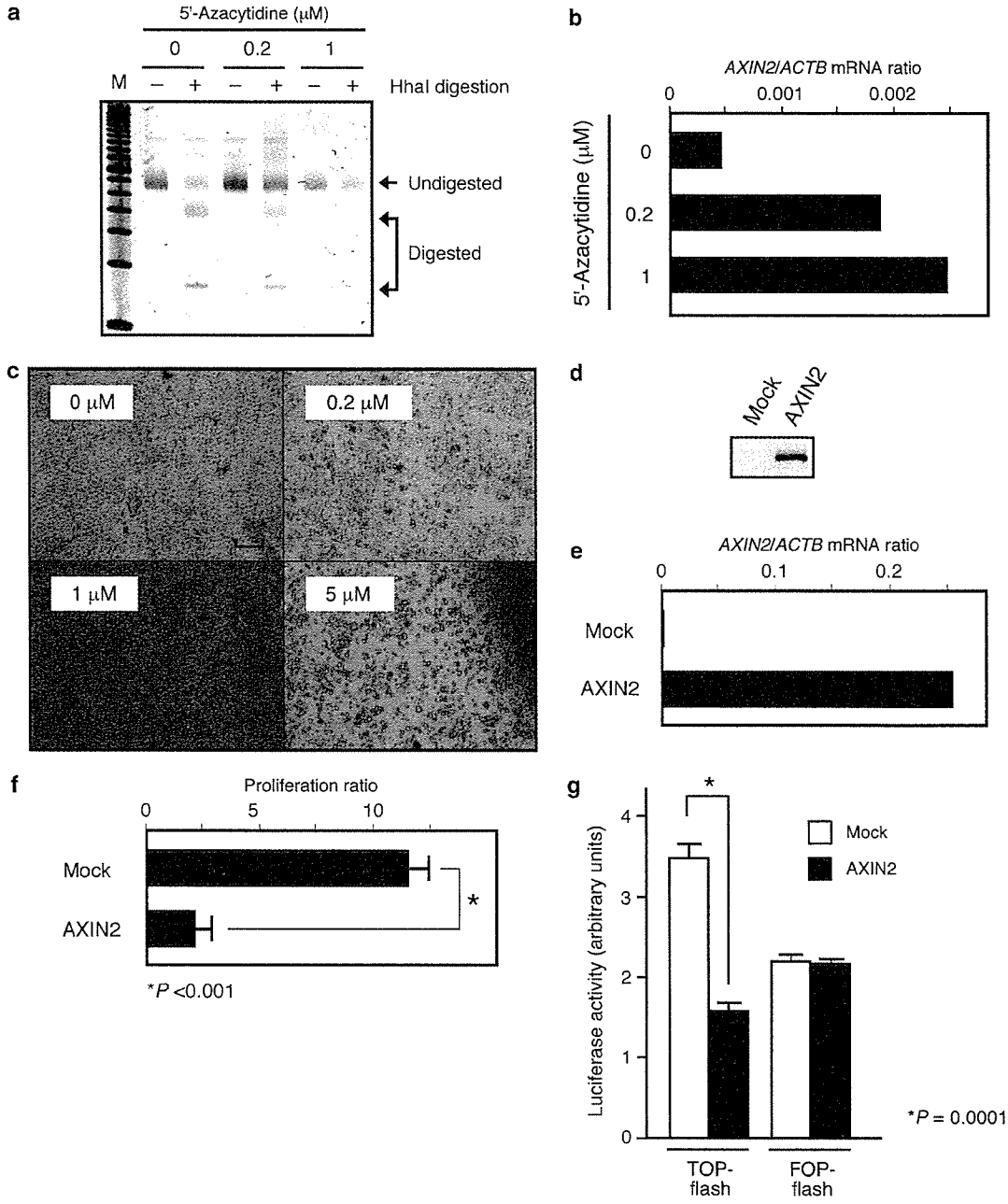

Acknowledgements

We thank M Toyota and SN Thibodeau for critical reading of the manuscript and helpful suggestions. This study was supported in part by a grant for Third-Term Comprehensive Control Research for Cancer from the Ministry of Health, Labor, and Welfare of Japan, and by a grant for 'High-Tech Research Center' Project for Private Universities: Matching Fund Subsidy (2002–2006) from the Ministry of Education, Culture, Sports, Science, and Technology of Japan.

References

Alon U, Barkai N, Notterman DA, Gish K, Ybarra S, Mack D *et al.* (1999). *Proc Natl Acad Sci USA* **96**: 6745–6750.

Behrens J, Jerchow BA, Wurtele M, Grimm J, Asbrand C, Wirtz R *et al.* (1998). *Science* **280**: 596–599.

Boland CR, Thibodeau SN, Hamilton SR, Sidransky D, Eshleman JR, Burt RW *et al.* (1998). *Cancer Res* **58**: 5248–5257.

Bronner CE, Baker SM, Morrison PT, Warren G, Smith LG, Lescoe MK *et al.* (1994). *Nature* **368**: 258–261.

Christman JK. (2002). *Oncogene* **21**: 5483–5495.
Cunningham JM, Christensen ER, Tester DJ, Kim CY, Roche PC, Burgart LJ *et al.* (1998). *Cancer Res* **58**: 3455–3460.
Esteller M, Sparks A, Toyota M, Sanchez-Cespedes M, Capella G, Peinado MA *et al.* (2000). *Cancer Res* **60**: 4366–4371.
Fellenberg K, Hauser NC, Brors B, Neutzner A, Hoheisel JD, Vingron M. (2001). *Proc Natl Acad Sci USA* **98**: 10781–10786.
Fishel R, Lescoe MK, Rao MR, Copeland NG, Jenkins NA, Garber J *et al.* (1993). *Cell* **75**: 1027–1038.
Ionov Y, Peinado MA, Malkhosyan S, Shibata D, Perucho M. (1993). *Nature* **363**: 558–561.
Issa JP. (2004). *Nat Rev Cancer* **4**: 988–993.
Kinzler KW, Vogelstein B. (1996). *Cell* **87**: 159–170.
Koinuma K, Shitoh K, Miyakura Y, Furukawa T, Yamashita Y, Ota J *et al.* (2004). *Int J Cancer* **108**: 237–242.
Korinek V, Barker N, Morin PJ, van Wichen D, de Weger R, Kinzler KW *et al.* (1997). *Science* **275**: 1784–1787.
Lengauer C, Kinzler KW, Vogelstein B. (1998). *Nature* **396**: 643–649.
Leung JY, Kolligs FT, Wu R, Zhai Y, Kuick R, Hanash S *et al.* (2002). *J Biol Chem* **277**: 21657–21665.
Liu W, Dong X, Mai M, Seelan RS, Taniguchi K, Krishnadath KK *et al.* (2000). *Nat Genet* **26**: 146–147.
Miyakura Y, Sugano K, Konishi F, Ichikawa A, Maekawa M, Shitoh K *et al.* (2001). *Gastroenterology* **121**: 1300–1309.
Narayan S, Roy D. (2003). *Mol Cancer* **2**: 41.
Ohki-Kaneda R, Ohashi J, Yamamoto K, Ueno S, Ota J, Choi YL *et al.* (2004). *Biochem Biophys Res Commun* **320**: 1328–1336.
Papadopoulos N, Nicolaides NC, Wei YF, Ruben SM, Carter KC, Rosen CA *et al.* (1994). *Science* **263**: 1625–1629.
Rajagopalan H, Lengauer C. (2004). *Nature* **432**: 338–341.
Rubinfeld B, Robbins P, El-Gamil M, Albert I, Porfiri E, Polakis P. (1997). *Science* **275**: 1790–1792.
Satoh S, Daigo Y, Furukawa Y, Kato T, Miwa N, Nishiwaki T *et al.* (2000). *Nat Genet* **24**: 245–250.
Smith G, Carey FA, Beattie J, Wilkie MJ, Lightfoot TJ, Coxhead J *et al.* (2002). *Proc Natl Acad Sci USA* **99**: 9433–9438.
Suzuki H, Watkins DN, Jair KW, Schuebel KE, Markowitz SD, Dong Chen W *et al.* (2004). *Nat Genet* **36**: 417–422.
Tolwinski NS, Wieschaus E. (2004). *Trends Genet* **20**: 177–181.
Toyota M, Ahuja N, Ohe-Toyota M, Herman JG, Baylin SB, Issa JP. (1999). *Proc Natl Acad Sci USA* **96**: 8681–8686.
Veigl ML, Kasturi L, Olechnowicz J, Ma AH, Lutterbaugh JD, Periyasamy S *et al.* (1998). *Proc Natl Acad Sci U S A* **95**: 8698–8702.
Wheeler JM, Beck NE, Kim HC, Tomlinson IP, Mortensen NJ, Bodmer WF. (1999). *Proc Natl Acad Sci USA* **96**: 10296–10301.
Wu R, Zhai Y, Fearon ER, Cho KR. (2001). *Cancer Res* **61**: 8247–8255.
Xiong Z, Laird PW. (1997). *Nucleic Acids Res* **25**: 2532–2534.
Yamashita Y, Kajigaya S, Yoshida K, Ueno S, Ota J, Ohmine K *et al.* (2001). *J Biol Chem* **276**: 39012–39020.
Zysman M, Saka A, Millar A, Knight J, Chapman W, Bapat B. (2002). *Cancer Res* **62**: 3663–3666.

Supplementary Information accompanies the paper on Oncogene website (http://www.nature.com/onc).

Oncology Research, Vol. 16, pp. 85–95

0965-0407/06 $90.00 + .00
E-ISSN 1555-3906
www.cognizantcommunication.com

Schedule-Dependent Interactions Between Pemetrexed and Cisplatin in Human Carcinoma Cell Lines In Vitro

Yasuhiko Kano,* Miyuki Akutsu,* Saburo Tsunoda,* Tohru Izumi,* Hiroyuki Kobayashi,* Koichi Inoue,† Kiyoshi Mori,‡ Hirofumi Fujii,‡ Hiroyuki Mano,§ Tsogbadrakh Odgerel,¶ and Yusuke Furukawa¶

*Division of Hematology, Tochigi Cancer Center, 4-9-13, Yonan, Utsunomiya, Tochigi, 320-0834, Japan
†Division of Radiation Oncology, Tochigi Cancer Center, 4-9-13, Yonan, Utsunomiya, Tochigi, 320-0834, Japan
‡Division of Medical Oncology, Tochigi Cancer Center, 4-9-13, Yonan, Utsunomiya, Tochigi, 320-0834, Japan
§Division of Functional Genomics, Jichi Medical School, 3311-1, Minamikawachi, Tochigi, 329-0431, Japan
¶Division of Stem Cell Regulation, Jichi Medical School, 3311-1, Minamikawachi, Tochigi, 329-0431, Japan

(Submitted July 1, 2005; revision received December 26, 2005; accepted January 10, 2006)

The combination of pemetrexed and cisplatin shows good clinical activity against mesothelioma and lung cancer. In order to study the potential cellular basis for this, and provide leads as to how to optimize the combination, we studied the schedule-dependent cytotoxic effects of pemetrexed and cisplatin against four human cancer cell lines in vitro. Tumor cells were incubated with pemetrexed and cisplatin for 24 h at various schedules. The combination effects after 5 days were analyzed by the isobologram method. Both simultaneous exposure to pemetrexed and cisplatin for 24 h and sequential exposure to cisplatin for 24 h followed by pemetrexed for 24 h produced antagonistic effects in human lung cancer A549, breast cancer MCF7, and ovarian cancer PA1 cells and additive effects in colon cancer WiDr cells. Pemetrexed for 24 h followed by cisplatin for 24 h produced synergistic effects in MCF7 cells, additive/synergistic effects in A549 and PA1 cells, and additive effects in WiDr cells. Cell cycle analysis of MCF7 and PA1 cells supported these findings. Our results suggest that the simultaneous clinical administration of pemetrexed and cisplatin may be suboptimal. The optimal schedule of pemetrexed in combination with cisplatin at the cellular level is the sequential administration of pemetrexed followed by cisplatin and this schedule is worthy of clinical investigations.

Key words: Pemetrexed; Cisplatin; Isobologram; Synergism; Antagonism

INTRODUCTION

Pemetrexed (multitargeted antifolate) is a novel antifolate that inhibits multiple points in folate metabolism including thymidylate synthase, dihydrofolate reductase, and glycinamide ribonucleotide formyl transferase (1–3). Preclinical studies of pemetrexed have demonstrated antitumor activity against a variety of human cancer cells in preclinical models (4). The optimal dose and schedule of pemetrexed was considered to be 500 mg/m^2 in a 10-min infusion once every 3 weeks (5,6). Clinical trials of pemetrexed showed a broad activity against a variety of solid tumors including malignant mesothelioma, and colorectal, pancreas, lung, head and neck, gastric, bladder, and breast cancers (6–14). Dose-limiting toxicities included neutropenia, mucositis, diarrhea, and severe nausea and vomiting (5,6). Patients with a folate-deficient state were associated with severe toxicity, and folate and cobalamin administration before pemetrexed has been introduced in clinical trials (9,13).

Combination chemotherapy has become a standard in the treatment of cancer, based upon theoretical advantages and on proven clinical efficacy. The clinical studies of pemetrexed and platinums (e.g., cisplatin, carboplatin, and oxaliplatin) in combinations have been used against malignant mesothelioma and non-small cell lung cancer, and the promising activity of this combination has been observed (15–19). The wide range of antitumor activity of pemetrexed and platinums (20), their different cytotoxic mechanisms and different toxic profiles, and the absence of cross-resistance provide a rationale for using combinations of these agents.

The cytotoxic action of cisplatin is considered to be the result of the formation of cisplatin–DNA adducts

Address correspondence to Yasuhiko Kano, Division of Hematology, Tochigi Cancer Center, Yonan 4-9-13, Utsunomiya, Tochigi, 320-0834, Japan. Tel: 011-81-28-658-5151; Fax: 011-81-28-658-5488; E-mail: ykano@tcc.pref.tochigi.jp